

Faculty and Staff Publication:

**Brendan O'Brien, Michael Rizzolo, Luke Prestowitz, and
Kathleen Dunn**

Citation for Final Published Published Work:

O'Brien, B. B., Rizzolo, M., Prestowitz, L. C., & Dunn, K. k. (2015). Rapid trench initiated recrystallization and stagnation in narrow Cu interconnect lines. *Applied Physics Letters*, 107(17), 1-5. DOI: 10.1063/1.4932577

Link to Publisher Site:

<http://aip.scitation.org/doi/10.1063/1.4932577>

Rapid trench initiated recrystallization and stagnation in narrow Cu interconnect lines

Brendan B. O'Brien, Michael Rizzolo, Luke C. Prestowitz, and Kathleen A. Dunn^{a)}

Colleges of Nanoscale Science and Engineering, SUNY Polytechnic Institute, Albany, New York 12203, USA

(Received 20 August 2015; accepted 25 September 2015; published online 30 October 2015)

Understanding and ultimately controlling the self-annealing of Cu in narrow interconnect lines has remained a top priority in order to continue down-scaling of back-end of the line interconnects. Recently, it was hypothesized that a bottom-up microstructural transformation process in narrow interconnect features competes with the surface-initiated overburden transformation. Here, a set of transmission electron microscopy images which captures the grain coarsening process in 48 nm lines in a time resolved manner is presented, supporting such a process. Grain size measurements taken from these images have demonstrated that the Cu microstructural transformation in 48 nm interconnect lines stagnates after only 1.5 h at room temperature. This stubborn metastable structure remains stagnant, even after aggressive elevated temperature anneals, suggesting that a limited internal energy source such as dislocation content is driving the transformation. As indicated by the extremely low defect density found in 48 nm trenches, a rapid recrystallization process driven by annihilation of defects in the trenches appears to give way to a metastable microstructure in the trenches. © 2015 AIP Publishing LLC. [<http://dx.doi.org/10.1063/1.4932577>]

As feature dimensions have continued to scale downward, copper interconnects have been plagued by undesirably high resistivity and short electromigration lifetimes due to the persistence of a polygranular microstructure.^{1–3} These Cu lines are formed using the damascene process, where patterns are etched into a dielectric film and coated (typically) with a TaN diffusion barrier, Ta adhesion layer, and Cu (or Cu alloy) seed layer. The lines are then overfilled with Cu by electrochemical deposition (ECD), yielding void-free lines with a continuous overburden layer on top of the features.⁴ The ECD of Cu into narrow geometries requires a high nucleation density, yielding a deposit with an extremely fine as-plated microstructure which can transform spontaneously at room temperature (“self-annealing”). Historically, this uncontrolled process was circumvented using a modest thermal anneal to encourage grain coarsening, yielding large columnar grains in the overburden. In wide (>100 nm) lines, this process resulted in large bamboo-type grains,^{5,6} but in narrow lines (<100 nm) the process stagnates, leaving the polygranular microstructure which is detrimental to performance. This dilemma has contributed to a re-evaluation of production targets, resulting in less aggressive scaling of back end of the line (BEOL) feature sizes than had been predicted just a few years ago.^{7–9}

Traditionally, the microstructural transformation of the ECD Cu deposited onto patterned substrates was thought to begin at the free surface of the overburden and progress down into the lines.¹⁰ Several publications, however, have suggested that in narrow lines, high dislocation density, seed layer texture, and minimization of the Cu-Ta interfacial energy cause coarsening of grains in the trenches prior to the overburden.^{8,11,12} In this work, TEM analysis of samples during and after the transformation is presented supporting

the trench-initiated recrystallization hypothesis, and goes further to show that the microstructure inside the trenches is stable well before the transformation in the overburden is complete.

Process of record (POR) wafers with patterned dielectric coated with iPVD TaN, Ta, and Cu seed layer were obtained from the State University of New York (SUNY) Polytechnic Institute’s Colleges of Nanoscale Science and Engineering (CNSE) 300 mm process line. Wafer coupons were mounted onto a rotating disk electrode using a custom wafer coupon holder described previously.¹³ Samples were electroplated using from a 3-component ATMI Enthone plating solution using a hot entry technique where the coupons were held at constant voltage to prevent etching of the seed layer. Upon entry, the flow of current triggered the power supply to switch to galvanostatic plating at 5 mA/cm² for trench fill and 50 mA/cm² for overburden deposition, targeting a 1000 nm overburden thickness.

For the case of room temperature annealing, the plated sample was taken from the electroplating bath and placed directly into the sample chamber of the FEI NovaLab 600 Dual Beam for TEM lamella preparation. This preparation—the extraction of a lamella and thinning to electron transparency—takes approximately 1.5 h. As such, this sample represents the closest to the true as-plated microstructure as we can achieve in this sample set. In many previous studies, a sample similar to this is considered the as-plated microstructure, but given the rapidity of the transformation, these samples can only represent a *nominal version* of the as-plated microstructure. Subsequent lamellas taken at various time points, measured in hours after plating, were taken from the same field of lines but at a distance of at least 500 μm away from the previous extraction sites to avoid any influence from stress relief, damage, or sputter-redeposition due to the previous FIB cuts.

Samples for elevated annealing experiments were taken directly from the plating station and placed in an annealing

^{a)} Author to whom correspondence should be addressed. Electronic mail: kdunn1@sunypoly.edu

furnace pre-heated to 250 °C with N₂ gas flow, with the exception of the initial $t = 0$ specimen which was placed in liquid nitrogen to prevent unwanted transformation. Samples were removed from the annealing furnace at intervals spanning 2 to 60 min, allowed to cool under N₂ gas for 2 min, then quenched and stored in liquid nitrogen to prevent further transformation. Each sample was later removed from the liquid nitrogen individually and TEM lamellae were extracted. Each lamella took 1.5 h from the time it was taken out of the liquid nitrogen until it was thinned to electron transparency.

TEM lamellae were imaged on either a JEOL 2010F 200 kV field emission TEM or an FEI Titan³ 300 kV field emission TEM. For grain size measurements, a panoramic TEM image was compiled by stitching together several images taken along the lamella. To ensure that all grains could be identified by diffraction contrast, each lamella was imaged at 3 tilt angles: along the Si 110 zone axis, +3° around an arbitrary axis, and -3° around an axis perpendicular to the first. These three conditions are chosen in order to discriminate between grains of similar but not identical orientation. In order to separate the behavior of the overburden from the features, a subset of grains was identified for analysis based on their location relative to the Ta liner. Only grains inside the trench or touching the Ta adhesion layer were traced manually from the on-axis montage. This tracing was compared to the off-axis images to ensure all grains were identified and counted. After tracing was complete, the area of each grain was measured using the Fiji version of Image J image analysis software.¹⁴ Once the area of each grain was determined, the equivalent grain diameter could be calculated and plotted.

Electron backscatter diffraction (EBSD) maps were obtained using a transmission EBSD (tEBSD) technique developed by NIST¹⁵ using the FEI NovaLab 600 Dual Beam equipped with a HKL Nordlys EBSD detector. tEBSD allows crystallographic orientation mapping of a TEM lamella with 10 nm resolution, a significant improvement over the 20–100 nm resolution usually associated with EBSD.¹⁵

Figure 1(a) shows a bright field TEM image of a lamella extracted from the wafer and thinned to electron transparency within 3 h of plating. In this image, two large grains, indicated with arrows, are seen touching the Cu/Ta liner interface while the rest of the overburden is still untransformed. This evidence supports the hypothesis that the trenches initiate transformation of the Cu microstructure, as previously suggested by our group and others.^{8,11}

The crystallographic orientation of these trench initiated grains with respect to the trench sidewall can indicate a potential underlying driving force which caused them to grow. Figure 1(b) shows the crystal orientation maps of these trench initiated grains, color coded (see stereographic triangle as key) according to the crystal direction normal to the sidewall. This direction (i.e., perpendicular to the copper/liner interface) is analogous to mapping the wafer normal in a Cu film. Typically in blanket films, the 111 direction of copper aligns normal to film surface; this texture development has been attributed to the minimization of Cu surface energy.^{16,17} For trench-initiated subsurface grains, however,

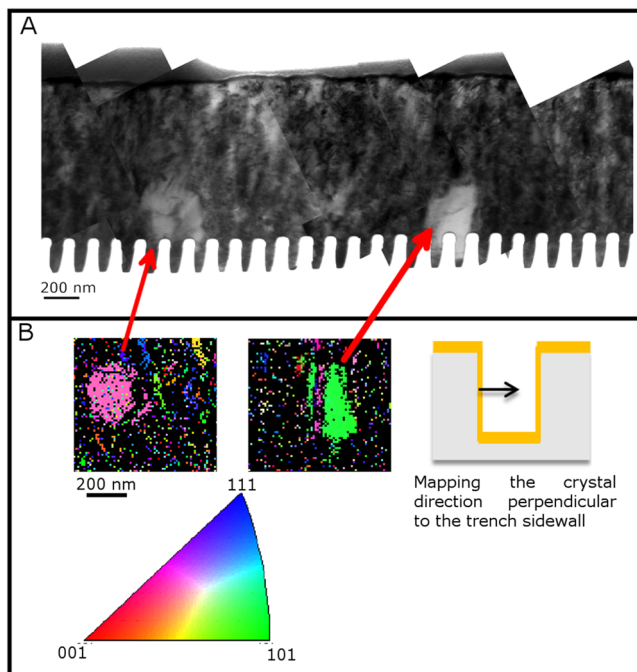


FIG. 1. Trench initiated grain coarsening. (a) Bright field TEM image of ECD Cu deposited in 70 nm lines after 3 h at room temperature showing two large grains (red arrows) growing from the trenches up into the overburden. (b) Transmission EBSD was used to map the crystallographic orientation of these large grains with respect to the trench sidewall normal.

the surface energy seems an unlikely driving force; here, the energy of the Cu-Ta interface has a stronger influence. Minimization of the Cu-Ta interfacial energy has been hypothesized to cause 111 texture normal to the trench sidewall.⁸ From the maps shown in Figure 1(b), however, it is evident that this is not the case. Instead, the emergence of arbitrarily oriented grains is the result of some other energy reduction process occurring quite rapidly in the trench.

To further explore the transformation of the microstructure in even narrower (48 nm) lines, diffraction contrast TEM images of the “as-plated” and annealed samples (both room temperature and 250 °C), as a function of annealing time were obtained. Figure 2(a) shows a bright field TEM image of the nominally “as plated” sample. This specimen was extracted as soon as possible after electroplating, but because TEM lamella extraction takes time (~1.5 h), some transformation may already have occurred. In this image, large grains, about the size of the trench width (labeled I-V), are already present. Some of the large grains, such as grain II or V which occupy the entire trench width, also have straight grain boundaries. Both of these microstructural features are not expected in the as-plated microstructure and indicate that some transformation has already occurred during the 1.5 h needed for TEM sample preparation.

Figure 2(b) shows the grain size distribution of Cu grains inside the trench and/or touching the Ta adhesion layer, as a function of time at room temperature. Figure 2(c) shows the analogous data as a function of time held at 250 °C. In these graphs, the grain equivalent diameter is plotted on the x-axis and the cumulative probability is plotted on the y-axis. The vertical line in the plot represents the minimum size of a bamboo grain in a 48 nm line. Comparing the

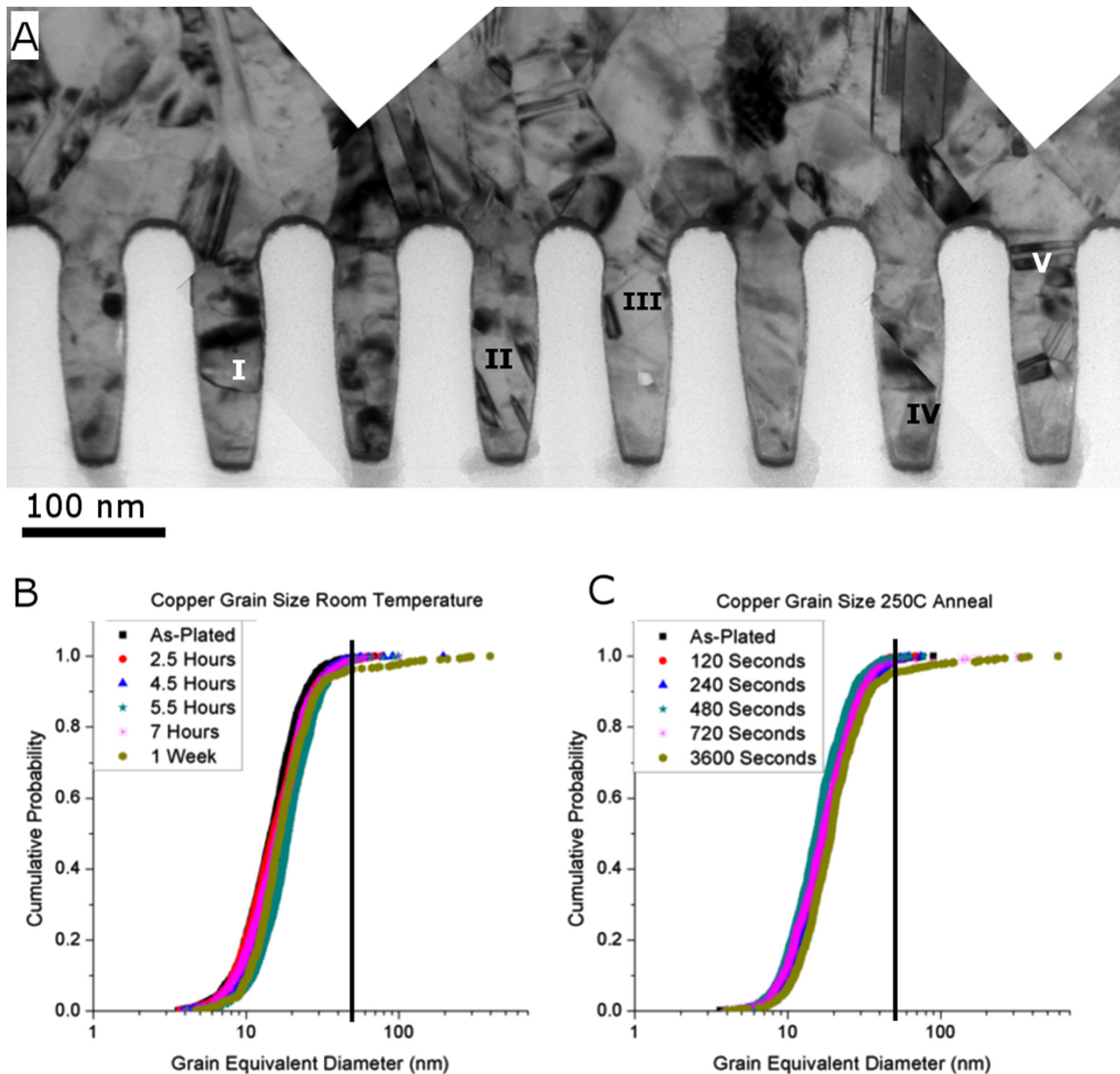


FIG. 2. Transformation of ECD copper in 48 nm lines. (a) Bright field TEM image after 1.5 h at room temperature (nominally as-plated). In this image, selected grains which span the entire trench have been marked with roman numerals to highlight the presence of these large grains. (b) Grain size distribution of self-annealed and (c) 250 °C annealed samples as a function of time. Only grains contained within the lines or touching the Ta adhesion layer are included.

as-plated curve with the most aggressive thermal budgets (either 1 week/room temperature or 1 h/250 °C), remarkably little changes. At the low end of the curves (below the 50% mark), there is little coarsening of the grains within the trenches, suggesting that the first 1.5 h at room temperature during lamella preparation is already long enough for the trench microstructure to have stabilized.

At the high end of the distribution, there is an increase in the number of large grains (>48 nm equivalent diameter) for the longer annealing times. These cumulative probability curves, however, mask the location of such growing grains. From the TEM images, it is clear that the grains at this end of the distribution correspond to the growth of grains from the field region and/or top of the trenches into the overburden (while still maintaining contact with the Ta liner), as seen in Figure 1. In other words, these large grains are not truly “in”

the trenches, although the growth appears to have initiated within the trench.

Finally, comparison of the grain size distributions for room temperature and 250 °C anneals shows that the microstructure in the trenches is similar for both temperatures. The insensitivity of the final grain size in the trenches to annealing temperature departs from the expected transformation behavior of Cu where the anneal temperature typically has a strong impact on final grain size.^{6,18} This departure, however, supports a transformation mechanism where internal stored energy such as deposition strain and dislocations are the dominant energies driving the transformation. The growth of defect-free grains will continue as long as the matrix still has an internal energy source to drive the transformation, and stops once the internal stored energy is consumed, as in a deformed metal film. Such an on/off type

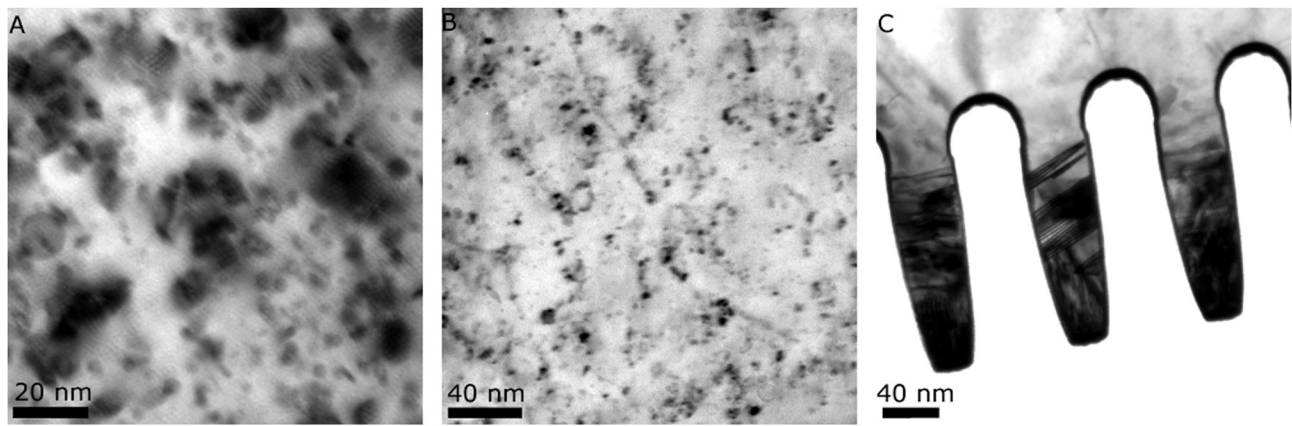


FIG. 3. Bright field TEM images showing the defect density in the overburden over 48 nm lines (a), inside a 1000 nm line (b), and inside 48 nm lines (c). There are fewer defects in the 48 nm lines than in the overburden or in a 1000 nm line.

of transformation with stored internal energy as a driving force implies that recrystallization rather than traditional grain growth is occurring in the trenches.^{19–21}

Additional evidence of recrystallization can be found in the internal structure of the grains themselves, since a hallmark of a post-recrystallization microstructure is the widespread appearance of grains with few internal defects.¹⁹ A side-by-side comparison of grain interiors of our samples is shown in Figure 3, with bright field diffraction contrast TEM images of the Cu microstructure in (a) the overburden, (b) a 1000 nm wide line, and (c) several 48 nm lines, recorded under identical imaging conditions (Si (110) zone axis, and 30 μm objective aperture). The speckled contrast in (a) and (b) indicates the presence of a significant number of dislocations not seen in (c). In the overburden over 48 nm lines, the defect density was found to be $\sim 1 \times 10^{12} \text{ cm}^{-2}$, which is similar to defect densities typically associated with ECD Cu films.⁵ The defect density in the 1000 nm lines was uniform across the trench with a value of $\sim 9 \times 10^{11}$, essentially the same as the overburden, consistent with the expectations for overburden-dominated transformation which has been widely reported for wide lines.¹⁰ In the narrow lines, assuming they had a defect density similar to the overburden, each 48 nm trench should have 90 to 100 dislocations per 100 nm in length (approximately the thickness of the TEM specimen). However, the copper in Figure 3(c) does not contain 90–100 dislocations per trench. In fact, many of the grains in the 48 nm trenches are defect-free, as would be expected in a fully recrystallized microstructure, adding strong evidence that recrystallization has gone to completion in the 48 nm trenches.

This situation raises the complementary question for the wide lines and overburden—if recrystallization explains the lack of dislocations in the 48 nm lines, why doesn't the same process result in a similarly low defect density in the overburden and in the 1000 nm lines? Theoretical calculations had suggested that the energy stored in defects densities of this magnitude was not enough to account for the abnormally large ($>5 \mu\text{m}$ diameter, in some cases) grains observed in the overburden.²² The presence of significant defect densities in our samples' overburden and 1000 nm lines even after aggressive annealing suggests that recrystallization, which minimizes stored internal energy (defects and deposition strain), is not driving the transformation. Instead, these results are consistent

with a transformation driven by grain growth to minimize interfacial energy (grain boundary and surface energy). Realistically, both energy reduction mechanisms may be operating simultaneously; it would appear, however, that different mechanisms dominate in different regions of the sample.

To explain the apparent trade-off between internal energy-driven recrystallization and interfacial energy-driven grain growth, we looked to the role of texture in transformation kinetics.²³ In our previous work,¹¹ we showed that the seed texture in narrow lines is random, while the field is still 111-textured, as would be expected in films. After plating, the overburden above the trenches is also 111-textured, despite the random orientations found on the sidewall seed.²⁴ These differences have important implications for transformation kinetics, according to the recent work on electroplated films. Several such studies using high resolution x-ray diffraction found that films deposited on untextured seed layers recrystallized faster than their textured counterparts, but resulted in smaller final grain size and lower final 111 texture. By extension, we expect that the untextured seed on the sidewall would lead to more rapid recrystallization in the trenches, while surface-initiated transformation of the textured overburden would be delayed. If, by the time the overburden grains grow, the recrystallization of Cu in the trenches has already reached a (meta)stable configuration, the overburden will be unable to convert the stable microstructure found in the trenches leaving the lines with an unfavorably polygranular microstructure.

In summary, support for the hypothesized trench-initiated grain coarsening from both 70 and 48 nm interconnect lines was presented. Additionally, it was shown that after the initial recrystallization of Cu in the 48 nm lines, the microstructure in the lines is stable, consisting of several dislocation-free grains. These results indicate that methods which retard the stabilization of the Cu microstructure in narrow trenches or which enhance the transformation rate of the overburden may give the overburden-initiated grain growth time to reach the bottom of the interconnect lines before they self-recrystallize, yielding interconnects with higher reliability and conductivity.

This research was funded by the Semiconductor Research Corporation Global Research Collaboration New York Center for Advanced Interconnect Science and Technology under Task 1292.083.

- ¹M. R. Baklanov, C. Adelmann, L. Zhao, and S. De Gendt, *ECS J. Solid State Sci. Technol.* **4**, Y1 (2014).
- ²B. Li, C. Christiansen, D. Badami, and C. C. Yang, *Microelectron. Reliab.* **54**, 712 (2014).
- ³M. Hauschildt, B. Hintze, M. Gall, F. Koschinsky, A. Preusse, T. Bolom, M. Nopper, A. Beyer, O. Aubel, G. Talut, and E. Zschech, *Jpn. J. Appl. Phys., Part 1* **53**, 05GA11 (2014).
- ⁴R. F. Yanda, M. Heynes, and A. K. Miller, *Demystifying Chipmaking* (Elsevier, Inc., 2005).
- ⁵J. M. E. Harper, C. Cabral, P. C. Andricacos, L. Gignac, I. C. Noyan, K. P. Rodbell, and C. K. Hu, *J. Appl. Phys.* **86**, 2516 (1999).
- ⁶P. R. Besser, E. Zschech, W. Blum, D. Winter, R. Ortega, S. Rose, M. Herrick, M. Gall, S. Thrasher, M. Tiner, B. Baker, G. Braeckelmann, L. Zhao, C. Simpson, C. Capasso, H. Kawasaki, and E. Weitzman, *J. Electron. Mater.* **30**, 320 (2001).
- ⁷S. Maitrejean, V. Carreau, O. Thomas, S. Labat, B. Kaouache, M. Verdier, J. Lepinoux, Y. Bréchet, M. Legros, J. Douin, S. Brandstetter, C. Cayron, O. Sicardy, D. Weygand, O. Dubreuil, and P. Normandon, in *Stress Induc. Phenom. Met. 10th Int. Work.*, edited by P. S. Ho, S. Ogawa, and E. Zschech (American Institute of Physics, 2009), pp. 135–150.
- ⁸K. J. Ganesh, A. D. Darbal, S. Rajasekhara, G. S. Rohrer, K. Barmak, and P. J. Ferreira, *Nanotechnology* **23**, 135702 (2012).
- ⁹International Technology Roadmap for Semiconductors 2011 Edition: Interconnect, 2011.
- ¹⁰V. Carreau, S. Maitrejean, Y. Brechet, M. Verdier, D. Bouchu, and G. Passemard, *Microelectron. Eng.* **85**, 2133 (2008).
- ¹¹B. B. O'Brien, E. Lifshin, and K. A. Dunn, *J. Electrochem. Soc.* **160**, D3139 (2013).
- ¹²C. Lingk and M. E. Gross, *J. Appl. Phys.* **84**, 5547 (1998).
- ¹³K. Ryan, K. Dunn, J. van Eijsden, and J. Adolf, *J. Electrochem. Soc.* **160**, D3186 (2013).
- ¹⁴J. Schindelin, I. Arganda-Carreras, E. Frise, V. Kaynig, M. Longair, T. Pietzsch, S. Preibisch, C. Rueden, S. Saalfeld, B. Schmid, J.-Y. Tinevez, D. J. White, V. Hartenstein, K. Eliceiri, and P. Tomancak, *Nat. Methods* **9**, 676 (2012).
- ¹⁵R. R. Keller and R. H. Geiss, *J. Microsc.* **245**, 245 (2012).
- ¹⁶C. E. Murray, R. Rosenberg, C. Witt, M. Treger, and I. C. Noyan, *J. Appl. Phys.* **113**, 203515 (2013).
- ¹⁷M. Treger, C. Witt, C. Cabral, C. Murray, J. Jordan-Sweet, R. Rosenberg, E. Eisenbraun, and I. C. Noyan, *J. Appl. Phys.* **113**, 214904 (2013).
- ¹⁸C. V. Thompson, *Annu. Rev. Mater. Res.* **30**, 159 (2000).
- ¹⁹P. G. Shewmon, *Transformations in Metals* (McGraw-Hill Book Company, 1969).
- ²⁰R. D. Doherty, D. A. Hughes, F. J. Humphreys, J. J. Jonas, D. Juul Jensen, M. E. Kassner, W. E. King, T. R. McNelley, H. J. McQueen, and A. D. Rollett, *Mater. Sci. Eng., A* **238**, 219 (1997).
- ²¹C. Detavernier, S. Rosnagel, C. Noyan, S. Guha, C. Cabral, and C. Lavoie, *J. Appl. Phys.* **94**, 2874 (2003).
- ²²H. Lee, W. D. Nix, and S. S. Wong, *J. Vac. Sci. Technol., B* **22**, 2369 (2004).
- ²³A. Ying, C. Witt, J. Jordan-Sweet, R. Rosenberg, and I. C. Noyan, *J. Appl. Phys.* **109**, 014907 (2011).
- ²⁴R. Rosenberg, D. C. Edelstein, C. Hu, and K. P. Rodbell, *Annu. Rev. Mater. Sci.* **30**, 229 (2000).

Applied Physics Letters is copyrighted by AIP Publishing LLC (AIP). Reuse of AIP content is subject to the terms at: <http://scitation.aip.org/termsconditions>. For more information, see <http://publishing.aip.org/authors/rights-and-permissions>.